Special Issue Article

Applied Organometallic Chemistry

Received: 8 March 2013 Revised: 18 June 2013 Accepted: 19 June 2013 Published online in Wiley Online Library: 27 August 2013

(wileyonlinelibrary.com) DOI 10.1002/aoc.3032

Cubic silsesquioxanes as tunable high-performance coating materials

Hyun Wook Ro[a], Vera Popova[b], Dave J. Krug[b], Aaron M. Forster[c], Richard M. Laine[b,d] and Christopher L. Soles[a]*

In this manuscript a series of cubic silsequioxane monomers with their eight vertices functionalized by different organic tethers and terminated with triethoxysilane groups were acid hydrolyzed, spin cast, and vitrified into hard organosilicate films. Both the length of the organic ligands and the number of triethoxysilane groups were varied to change the degree of cross-linking and cubic silsequioxane content of the vitrified films. This resulted in a series of high-quality optical-grade coatings with excellent properties. In general, higher concentrations of the cubic silsequioxane moiety in the network and higher cross-link densities led to enhanced mechanical properties, lower porosity, higher density, lower thermal expansion, and a very hydrophilic surface. The manner by which these properties can be tuned via the cubic silsesquioxane content is discussed in comparison to the structure–property relations for other spin on silsequioxane type films. Copyright © 2013 John Wiley & Sons, Ltd.

Keywords: silsequioxane; organosilicate; films; porosity; modulus; characterization

Introduction

Silsesquioxanes (SSQs) are a general class of inorganic–organic hybrid materials consisting of silicon atoms each coordinated with three bridging oxygen atoms. The basic chemical formula of these materials is $RSiO_{1.5}$, where R is an organic substituent. The oxygen atoms covalently link adjacent Si atoms, creating a cross-linked organosilicate network via Si–O–Si linkages.[1–4] Such SSQ materials are widely used in a range of thin film or coating applications, including nanocomposites, scratch-resistant coatings, barrier coatings, biological devices, separation media, optical films or coatings and semiconductor interconnect insulators.[1–11] This widespread interest stems from the fact that the SSQ precursors can be easily processed into smooth films using solution casting methods and then cross-linked into hard, transparent films at elevated temperatures. Some of their attractive attributes include the ease with which SSQs can be processed into optical-quality films and coatings, the capacity of these films and coatings to support high levels of porosity and capability of tailoring the surface chemistry of the inner wall of pores,[11,12] and their ability to withstand temperatures in excess of 400 °C and aggressive environments without thermal or chemical degradation. However, these attractive properties are often offset by poor mechanical properties. SSQ networks tend to be fragile due to the stresses that build up during their high-temperature vitrification process and are often not able to support mechanical loads without failure.[11,13] Furthermore, it can be difficult to obtain reproducible and well-controlled bounds on the mechanical properties of these cross-linked SSQ networks; their performance has been shown to be strongly linked not just to the initial monomer structure but also the synthetic conditions that determine the evolution of the intermediate oligomeric structures. These intermediate structures have a direct impact on the final properties of the material after vitrification. Recently we published two reports illustrating how the physical and mechanical properties of an SSQ film can be tuned by adjusting the processing parameters for a given organosilicate chemistry.[14,15]

The precursors for SSQs are typically trifunctional silanes such that each Si atom has three functional groups such as alkoxys or chlorines. These functional groups are typically converted into silanols (Si–OH) through a hydrolytic reaction in the presence of either an acidic or basic catalyst in water. The hydrolysis reaction promotes the formation inter- and/or intra- polycondensation reactions that lead to neighboring monomers being covalently connected via Si–O–Si linkages. It is understood that the hydrolytic polycondensation reaction mechanism can lead a variety of different microstructures, including randomly branched cross-linked networks, more regular ladder-type networks, or cage-like structures including partially and perfectly closed-cage molecules (see Fig. 1). Of the closed-cage structures, the most common form is usually the octameric SSQs, where eight Si atoms are covalently connoted via Si–O–Si linkages to form a perfect, single cube. Recent measurements show that significant enhancements in the modulus and hardness, along with a reduction in the coefficient of thermal expansion (CTE), can be achieved by biasing the reaction conditions to maximize the number of closed-cage and strained cyclic moieties in the final cross-linked SSQ network. This was achieved both by controlling the reaction and gelation times of the SSQ monomers as well as adding structure-guiding SSQ monomers to

* *Correspondence to: Christopher L. Soles, National Institute of Standards and Technology, Materials Science and Engineering Division, 100 Bureau Drive, Mail Stop 8541, Gaithersburg, MD 20899, USA. Email: csoles@nist.gov*

a *National Institute of Standards and Technology, Materials Science and Engineering Division, Gaithersburg, MD, 20899, USA*

b *Mayaterials Inc., Ann Arbor, MI, 47108, USA*

c *National Institute of Standards and Technology, Materials and Structural Systems Division, Gaithersburg, MD, 20899, USA*

d *Department of Materials Science and Engineering, University of Michigan, Ann Arbor, MI, 48104, USA*

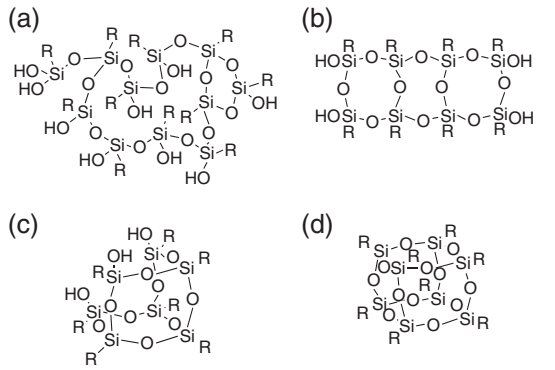

Figure 1. Different representative microstructures for an SSQ network: (a) random network; (b) ladder; (c) partial cage; (d) octameric cage (T8).

the reaction mixture.[14,15] A subtle but very important distinction is that a perfect cage structure where the organic R group is non-reactive will become isolated, forming a nanoparticle that cannot be bonded to the cross-linked network. These types of isolated cages do not improve physical properties because they usually sublime upon vitrification. R groups that can continue to react with the organosilicate network, however, should help facilitate better mechanical properties.

In this manuscript we focus on films prepared from perfect-cube, octameric SSQ monomers. These materials are designed to directly test the notion that retaining the closed-cage moieties in the cross-linked network is important for enhancing the mechanical properties. The corners of the cubes are functionalized by a series of organic substituents designed to vary the overall cross-link density and organic content of the film. The physical and mechanical properties of the resulting films are characterized in detail to evaluate the performance of the SSQ monomers in preparing robust coatings. The systematic variation in the chemical structure of the SSQ monomers and the detailed characterization methods introduced here will hopefully provide materials designers with the insight to develop improved SSQ materials.

Experimental

Film Preparation

The chemical structures of the different SSQ monomers used in this work are shown in Fig. 2. The synthetic details for preparing these monomers have been discussed previously in detail.[7] The as-received monomers (0.1–10.0 mmol) were added to a stirred THF (6 ml) solution in a 50 ml round-bottom flask. To this a mixture of distilled water (H_2O) and hydrochloric acid (HCl, 1 M) was added drop-wise while stirring at 0 °C. The molar ratio of the reaction mixture was 1:0.2:50 [SSQs:HCl:H_2O]. After stirring the reaction mixture for 24 h at room temperature, the reaction mixture was poured into a solvent system consisting of diethyl ether and water, resulting in a phase separation. The organic phase was recovered and stirred with magnesium sulfate ($MgSO_4$) for 30 min, followed by filtering through a 0.4 μm PTFE syringe filter. Solvent was slowly evaporated by a rotary evaporator. The remaining product was dissolved in propylene glycol propyl ether (PGPE) as the spin-casting solution. Films approximately 100–500 nm thick were spin cast on to clean Si wafers with a native oxide surface. The as-cast films were then heated to 400 °C in an inert N_2 environment to convert the oligomeric as-cast film into a hard, cross-linked SSQ network.

Thermogravimetric Analysis

TGA measurements were performed on a TGA Q500 (TA instruments[16]) with the samples, both the as-received and hydrolyzed materials, in an inert nitrogen atmosphere. The samples were dried at 60 °C under vacuum prior to testing and then thermally ramped in the TGA instrument to 500 °C at a heating rate of 10 °C min^{-1}. The mass loss as a function of temperature was recorded.

Nanoindentation

Depth-sensing indentation (DSI) measurements were conducted using the dynamic contact module (DCM) on an MTS NanoIndenter. All films were 500 nm thick and indented to a maximum depth of 50 nm in order to minimize substrate effects. Twenty indents were conducted on each sample and the average modulus and hardness were reported from these data. A pyramidal Berkovich tip was used to indent the samples. The tip shape function was determined through 100 nm depth indents into fused silica. The contact stiffness between the sample and the indenter were measured as a function of indentation depth by imposing a 2 nm, 75 Hz oscillation over the programmed constant strain rate loading of 0.05 mn s^{-1}. The average modulus and hardness were determined for each indent over a depth range of 20–35 nm . The reported average modulus and hardness were determined from an average of 20 indents into each film.

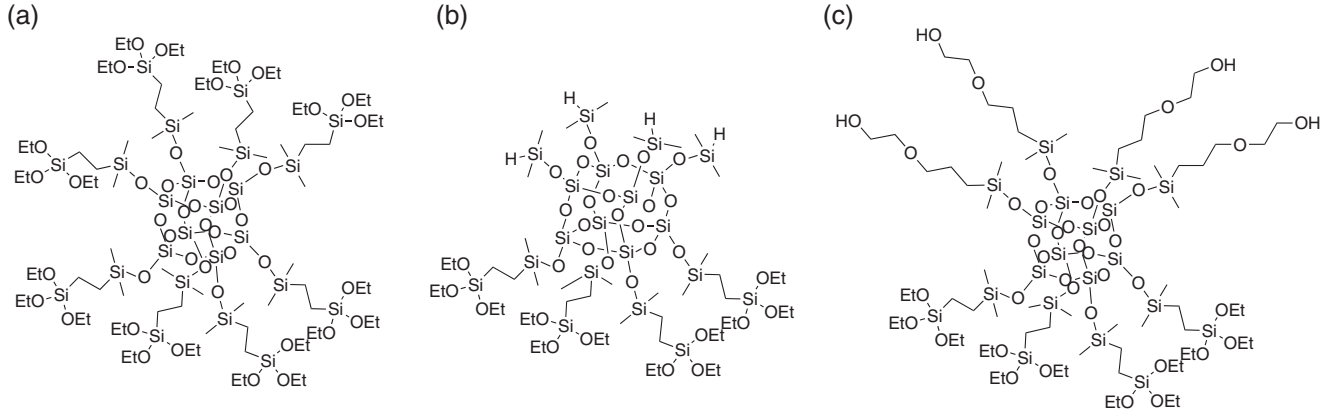

Figure 2. Chemical structures of the SSQ monomers used in this study: (a) octa(triethoxysilylethyl)(octadimethylsiloxy)octasilsesquioxane (OTSE); (b) [tetra (triethoxysilylethyl)dimethylsiloxy tetradimethylsiloxy)octasilsesquioxane (TTSE); (c) [tetra(triethoxysilylethyl)dimethylsiloxy][tetra(2-hydroxyethoxyethyl dimethylsiloxy]octasilsesquioxane (TOETSE).

Contact Angle Measurement

Contact angle measurements were made by the sessile drop technique using a Krüss G2 contact angle instrument with the sample held at room temperature. SSQ films were first annealed at different temperatures (as-cast, 100, 170, and 380 °C) under a nitrogen environment before the contact angle measurements. A deionized (DI) water droplet (approximately 2 μl volume) was deposited on the sample surface and the static equilibrium contact angle (CA) was measured immediately upon needle removal. The average of at least five measurements taken at different positions on each sample was reported contact angle.

Specular X-Ray Reflectivity (SXR)

SXR measurements were performed on a Philips X'PERT diffractometer using Cu-Kα X-ray radiation ($\lambda = 1.54$ Å). The incident beam was focused with a curved mirror into a 4-bounce Ge [220] crystal monochromator before being incident onto the sample. The reflected beam was further conditioned with a 3-bounce Ge [220] crystal monochromator to ensure the specular condition. The angular reproducibility of the goniometers that control the sample rotation and angular position of the X-ray detector was 0.0001°. The reflectivity was collected at 25 °C under vacuum for all samples.

Precision out-of-plane CTE measurements were made by measuring the thickness of the films as a function of temperature using SXR. The thickness of a film was determined from the spacing of the interference fringes. Planar SSQ films were placed in a specially designed vacuum chamber and the thickness was measured at four different temperatures: 25, 75, 125, and 175 °C. The reflectivity measurements were performed in a vacuum of 1×10^{-6} Pa after annealing the film at the predetermined temperature for 1 h. After the measurement at 175 °C, the samples were cooled to 25 °C and the measurements were repeated in order to confirm a reversible expansion and contraction behavior.

Once all the SXR data in the vacuum were collected, the sample chamber was purged with dry air saturated with toluene vapor. Toluene readily wets most SSQ materials and can easily absorb into the film, filling up any intrinsic porosity. By quantifying the scattering length density of the film in the vacuum and in the presence of the saturated toluene, we can quantify the porosity and densities of the film, including the average density and the wall density of material between pores. These types of X-ray porosimetry measurements have been described previously in greater detail.[17]

Results and Discussion

The chemical structures of the three different SSQs used in this study are shown in Fig. 2. They are all octameric SSQ cores decorated with various organic groups, including the important ($Si(OEt)_3$) functional ethoxy groups. The three different SSQ precursors in Fig. 2 were designed to establish structure–property relationships. Previously we reported that maximizing the number of closed-cage structures in the cross-linked network is important for enhancing mechanical properties like modulus or hardness[14,15]; the molecules depicted in Fig. 2 embrace this concept. The octa(triethoxysilylethyl)(octadimethylsiloxy)octasilsesquioxane (OTSE) is designed to maximize the number of functional end groups (24, as shown in Fig. 2a) and thus the cross-link density of the organosilicate network. The (b) [tetra (triethoxysilylethyl)dimethylsiloxy tetradimethylsiloxy)octasilsesquioxane (TTSE) and (c) [tetra(triethoxysilylethyl)dimethylsiloxy] [tetra(2-hydroxyethoxyethyl dimethylsiloxy]octasilsesquioxane (TOETSE) are bifunctional monomers that contain two distinctly different kinds of pendant groups.[7] In the TTSE case, four out of eight cage vertices are terminated by the $Si(OEt)_3$ functional groups while the remaining four are terminated by hydrolytically stable Si–H bonds (Fig. 2b). TOETSE contains the same four functional end groups as TTSE, but the other four corners are comprised of longer, more flexible organic tethers with simple hydroxyl end groups (Fig. 2c).

While the organic pendants render the SSQs soluble in a range of organic solvents that are suitable for spin-casting or solution processing into films, the TGA trace in Fig. 3 reveals that the as-received SSQs are not yet suitable for high-temperature vitrification processes. Upon heating these as-cast films, the SSQ molecules sublime, as evidenced by the significant mass loss near 300 °C. Similar measurements on octameric SSQs with non-reactive end groups such as alkyls also exhibit excessive mass loss in the range 250–500 °C due to sublimation, depending upon the kind and length of organic pendant group.[3,18] The SSQ monomers used in this study possess either Si–OEt, Si–H or C–OH terminal groups, which are susceptible to polycondensation

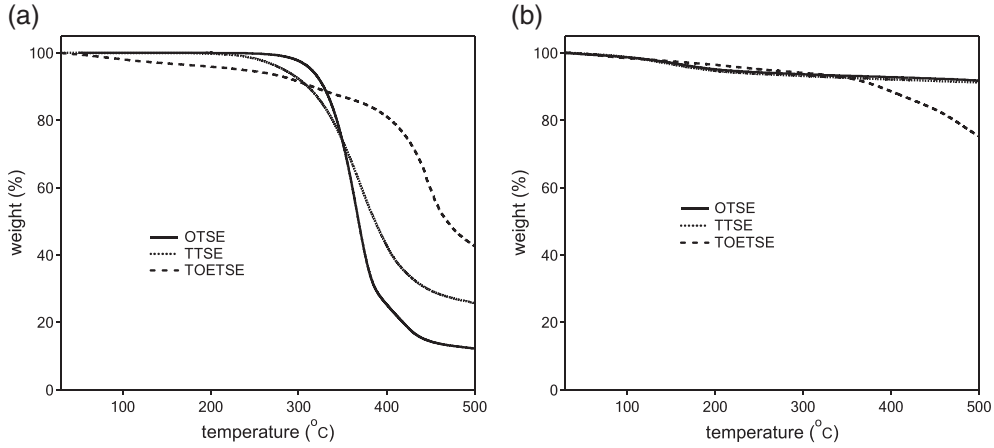

Figure 3. TGA traces of (a) as-received SSQ monomers showing significant mass loss, and (b) the same SSQ monomers after hydrolysis (with oligomerization).

reactions. However, these reactions are difficult in an inert environment for the SSQs and sublimation or evaporation is more likely to occur before the thermal polycondensation reaction takes place. Conversely, it has been shown for solid films in inert environments that the condensation cross-linking reaction occurs faster and at lower temperatures when the Si–OH content in the film is high.[19] To ensure cross-linking before sublimation it is important to maximize the Si–OH content; the thermal polycondensation reaction should occur before the sublimation, setting up an internal competition between the condensation cross-linking reaction and sublimation.

Simple sol–gel reactions are usually employed to oligomerize or polymerize the SSQs, and the reaction conditions, including the molar ratios of monomer/catalyst/water, type of solvent and reaction temperature, are all known to play a critical role in determining the microstructure of SSQs. We have found it is important to initiate the sol–gel reactions of these SSQ materials in the presence of an acid catalyst and an excess amount of water. Under these conditions the maximum amount of (Si–OEt)s is favorably converted into reactive silanol groups before the polycondensation reactions become dominant. The silanol groups are much more reactive than Si–OEt groups for thermal polycondensation reaction to form Si–O–Si linkages. As cross-linking in solution occurs, molecular mass will increase and lead to a decrease of the active silanol end groups. However, the polycondensation reaction can be retarded when the reaction is carried out with excess of water at low temperature. Under these conditions, the reaction products remain oligomeric ($M_W < 2000$ u) and most of the end groups tend to be silanols.

If these low-molecular-mass oligomers are collected from the acidic reaction solution soon enough, they can be redissolved in an organic solvent and spin cast into smooth films. The enriched silanol group content in these films significantly changes the TGA response of the material. At high silanol content the secondary condensation begins at low temperatures before sublimation sets in. This results in minimal mass loss for the hydrolyzed films, up to temperatures as high as 500 °C. The OTSE and TTSE films lose a small amount of material – approximately 9% by mass – which is consistent with the stoichiometric evolution of water from the secondary condensation reaction. Above 400 °C, the TOETSE shows a slightly greater mass loss than the other two compounds. We suspect that this is due to thermal degradation of the larger organic substituent at elevated temperatures. The shorter tethers in the OTSE and TTSE monomers are not thermally labile at high temperatures.

All of the as-cast organosilicate films had a mirror-smooth optical finish with very little roughness. When these films were heated to 400 °C to induce full cross-linking of the organosilicate material, the vitrified films retained their optically smooth appearance. Specular X-ray reflectivity (SXR) measurements were used to quantify the thickness and roughness of these films. Figure 4 shows the SXR data at several temperatures for both the OTSE and TOETSE films. The smoothness of the films is evident by the well-defined fringes at high Q, indicative of

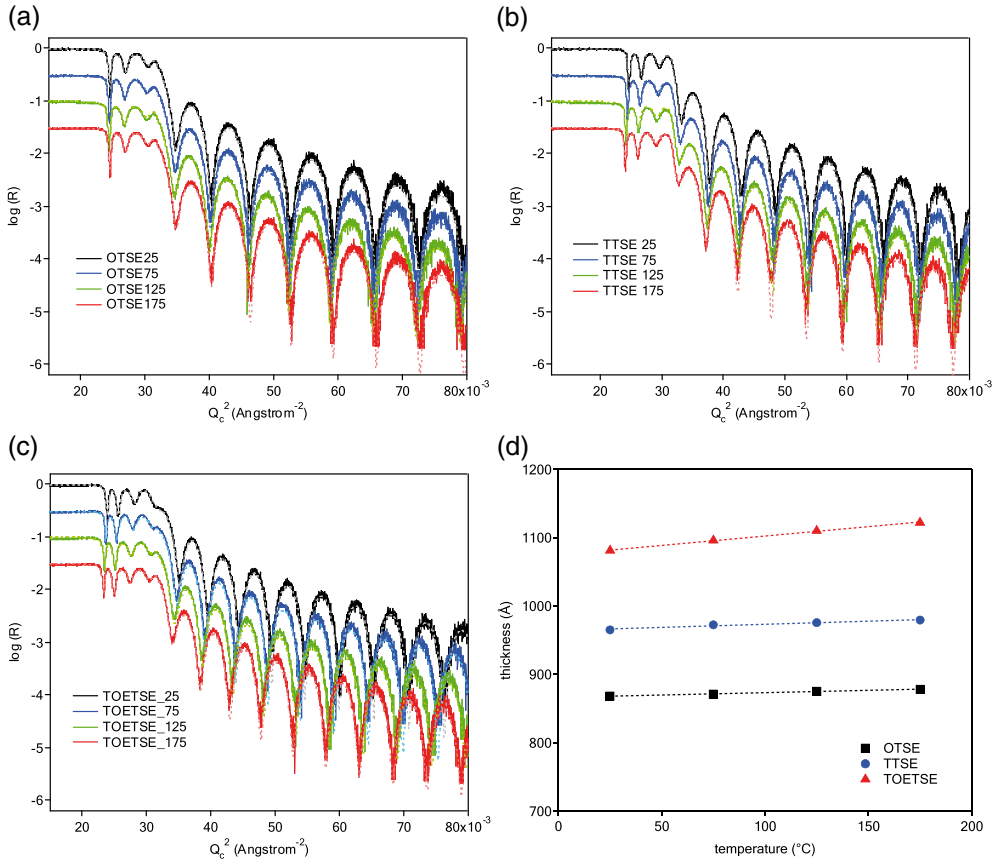

Figure 4. Experimental X-ray reflectivity data as a function of temperature (25, 75, 125, and 175 °C) for the vitrified SSQ films of (a) OTSE, (b) TTSE, and (c) TOETSE. Part (d) shows the evolution of film thickness with temperature with the linear fit used to quantify the CTE of the different films.

extremely low roughness. While we do not show the data here, a small amount of shrinkage is observed in the high-temperature vitrification process, but with very little change in roughness. These data show that high-quality optical grade films can be prepared from these engineered organosilicate materials.

The temperature dependence of the SXR data can be used to quantify the coefficient of thermal expansion (CTE) of the organosilicate films. As shown in Fig. 4, SXR data were recorded as a function of temperature between 25 and 175 °C. The thickness of the film is inversely proportional to the periodicity of the interference fringes in the reflectivity data. As the temperature increases, the period of oscillation of the fringes become increasingly compressed, indicative of expansion. A least squares multilayer fitting routine is used to quantify both the thickness and the roughness of the organosilicate films from the reflectivity data, with the fits provided in Fig. 4. A linear CTE is extracted from the temperature dependence of the thickness, normalized by the film thickness at 25 °C. As shown in Fig. 4(d), it is apparent that the TOETSE film exhibits the largest CTE. At $(274 \times 10^{-6})°C^{-1}$, the CTE of TOETSE is comparable to a typical polymeric material in the glassy state. At the other extreme, OTSE displayed the lowest CTE of the three, with a value of $(68 \times 10^{-6})°C^{-1}$; the CTE of the TTSE was intermediate, with a value of $(93 \times 10^{-6})°C^{-1}$.

In general, the trends in the CTE are consistent with the structural design cues previously reported[14,15] and the molecular variations of the monomers in Fig. 1. Increased incorporation of the closed-cage structures into the cross-linked networks leads to a strong reduction of the CTE. All of the cages here are designed to be incorporated into the network and the CTE decreases as the cross-link density increases surrounding the cage. It is tempting to argue that the glassy polymer-like CTE of TOETSE is consistent with the greater organic content of the long tethers on the corners of the octahedral SSQ core. However, it is important to remember that the TGA data suggest that the organic tethers on the TOETSE molecules are partially volatilized upon vitrification; the organic content is largely eliminated upon vitrification. In this respect the large CTE of the TOETSE either reflects a reduced cross-link density or an increased porosity. We return to this issue later in the discussion.

In addition to forming optically smooth films, all three materials exhibited excellent transparency in the visible spectrum. A set of the OTSE, TTSE, and TOETSE films were prepared on optical microscope slides under the same processing conditions as the films on the silicon substrate to quantify their absorption characteristic. Additionally, the OTSE material was prepared on a quartz slide to characterize the transparency further into the ultraviolet regime. For all of these optical measurements the film thickness was approximately 1 μm. Figure 5(a) compares the UV–visible absorption characteristics of the supporting optical microscope slide with the slides coated with the organosilicate films. The transmittances of the coated films are comparable to the bare glass substrate at a film thickness of approximately 1 μm. Figure 5(b) shows that this transparency is extended into the UV regime for OTSE, providing a quartz-like transparency. Only at wave numbers approaching 200 nm does OTSE become slightly more absorbent than quartz. Both the optical smoothness and transparency of these organosilicate materials make them attractive for optical grade coatings.

The porosities of the vitrified films were characterized using X-ray porosimetry (XRP). The SXR data for the CTE measurements were collected with the sample under vacuum. This was done to prevent gases or vapors from condensing in the intrinsic pores of the films. The XRP sample chamber was then filled with saturated toluene vapor. Under these conditions, the toluene capillary condensed into the nanoscale pores, filling the porosity. The infiltration of liquid toluene into the pores resulted in an appreciable change in the scattering length density of the film that was easily detected by SXR. Using the density of liquid toluene, it is straightforward to convert this increase in the scattering length density to a volume of toluene adsorbed into the pores, and thus the porosity.

Figure 6 shows the reflectivity data for OTSE and TOETSE films, both in vacuum and in the presence of saturated toluene (room temperatures data). The critical scattering length density for total external reflection of X-rays for the SSQ films is evidenced by the first strong minimum in the reflectivity data in the region of $Q = 0.025$ Å^{-1}. The condensation of toluene into the pores shifts this minimum to the right (higher Q), indicating an increase in film density as toluene condenses in the pores. The degree of shift is greater for the TOETSE film, indicating a higher level of porosity than the OTSE. The porosities of the vitrified OTSE, TTSE, and TOETSE films are 9.5%, 13.0%, and 15.0% by volume, respectively, as summarized in Table 1. It is notable that the porosity values track the CTEs reported above. The films with larger CTEs also display greater intrinsic porosity.

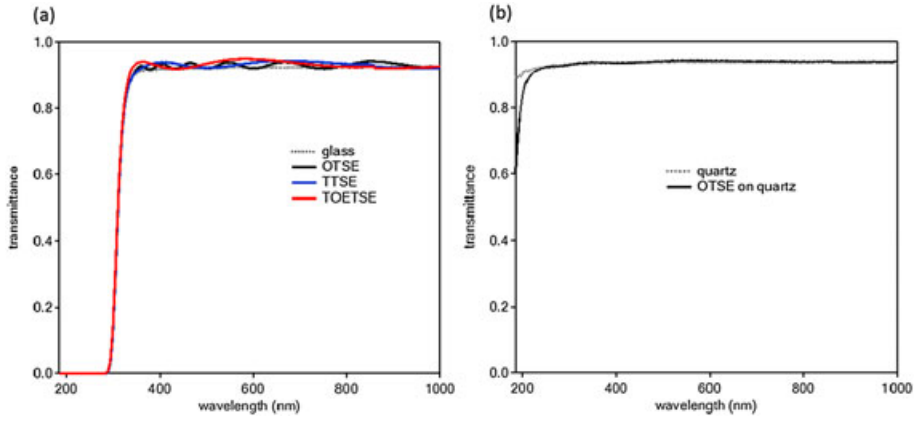

Figure 5. Part (a) compares the optical transmittance values for OTSE, TTSE, and TOETSE films supported on a glass substrate with that of the bare glass slide. Part (b) compares the optical transmittance values for a film of OTSE on a quartz substrate with the bare quartz substrate. These data show that in approximately 1 mm thick films these organosilicate materials are very transparent.

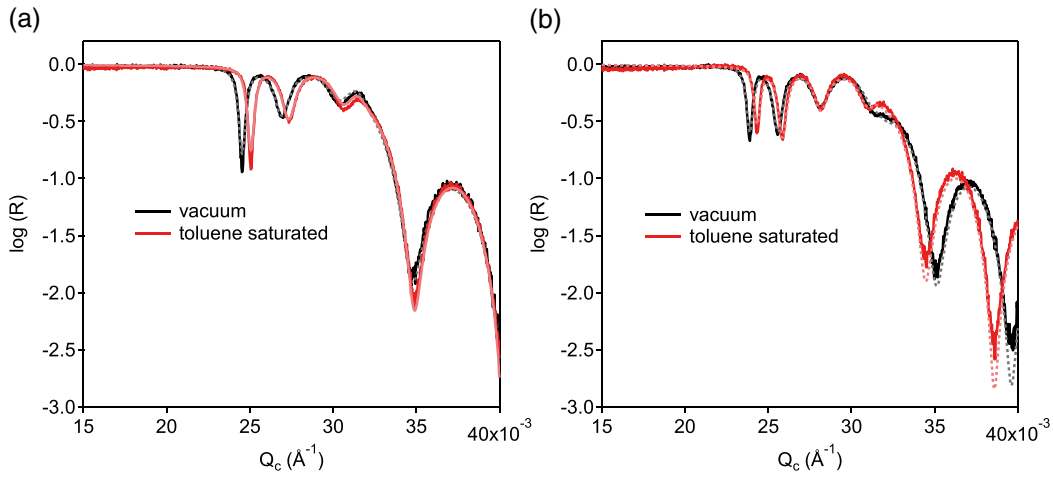

Figure 6. X-ray reflectivity data for the vitrified (a) OTSE and (b) TOETSE films under vacuum (black) and saturated toluene vapor (red). The density of the OTSE film appears to change when toluene is condensed inside the pores but the film thickness does not. However, TOETSE shows signs of both an increased density and swelling upon exposure to toluene vapor.

Table 1. Summary of the physical characteristics of fully vitrified films

Sample	T (°C)	d (Å)	ρ_{ave} (g cm^{-3})	ρ_{wall} (g cm^{-3})	P (%)	CTE ($\times 10^{-6}$ °C^{-1})	Modulus (GPa)
OTSE	25	868					
	75	871					
	125	875	1.232 ± 0.005	1.361 ± 0.005	9.5 ± 1.0	68 ± 5	5.8 ± 0.30
	175	878					
	Toluene	880					
TTSE	25	965					
	75	973					
	125	976	1.189 ± 0.005	1.367 ± 0.005	13.0 ± 1.0	93 ± 5	4.56 ± 0.07
	175	980					
	Toluene	985					
TOETSE	25	1081					
	75	1096					
	125	1110	1.129 ± 0.005	1.328 ± 0.005	15.0 ± 1.0	274 ± 5	2.14 ± 0.02
	175	1122					
	Toluene	1140					

The first two columns summarize the thickness d of the sample under vacuum at four different temperatures T plus when the pores are saturated with toluene at 25 °C. The temperature dependence of the thickness is used to calculate the linear coefficient of thermal expansion (CTE). ρ_{ave} and ρ_{wall} represent the average film density and density of materials between the pores, whereas P reflects the overall porosity quantified by X-ray porosimetry. The reduced modulus is determined from nanoindentation measurements as described in the text.

Analogous to thermal expansion, the X-ray reflectivity data can also be used to quantify solvent-induced swelling of the films. The critical scattering length density of the Si substrate on which these films reside is typically of the order of $Q = 0.032$ Å^{-1}. Between $Q = 0.025$ Å^{-1} and $Q = 0.032$ Å^{-1}, the X-rays wave guide through the SSQ film and become very sensitive to the film density. Beyond $Q = 0.032$ Å^{-1} the X-rays set up interference patterns from reflections off the air–SSQ and SSQ–substrate interfaces and become more sensitive to total film thickness. It is notable that beyond $Q = 0.032$ Å^{-1} the interference fringes for the OTSE films in the vacuum and toluene environments essentially overlap. This suggests that, while the film adsorbs toluene into its intrinsic pores, it does not swell. However, for the TOETSE film the interference fringes beyond $Q = 0.032$ Å^{-1} shift to the left. This suggests that in addition to increasing the density of the film, the adsorbed toluene also swells the TOETSE film. This is consistent with the increased CTE of TOETSE over OTSE; the material appears softer.

In addition to porosity and expansion, XRP can also be used to quantify the density of the film. The SXR measurements directly probe the scattering length density which, knowing the atomic composition, can be directly converted into a physical density. For the films in vacuum, the average density measured by SXR averages together the contributions from the intrinsic porosity of the material with the dense wall material 'between' the pores. As expected, Table 1 reveals that the average mass density of the films shows a quantitative correlation with the porosity. Films with a higher porosity display a lower average density. The condensation of toluene inside the pores shifts this density to

higher values by a well-defined amount. By knowing the magnitude of this shift and assuming the density of the condensed toluene is liquid-like, one can calculate the wall density of the material between the pores. The resulting wall densities, to a first approximation, are very similar for the three different materials (Table 1). This is a subtle but important distinction. It suggests that the changes in CTE (and other physical properties to be discussed below) are due to changes in porosity and not the physical properties of the material itself. The density of the solid phase between the pores remains essentially constant. The changes in the molecular architecture of the functional tethers in the octameric SSQ core impact the degree of packing and cross-linking through steric hindrances, but not the density of the solid phase itself. It also confirms the previous notion that very long non-reactive organic tethers in the TOETSE molecule start to act as porogens that volatilize upon conversion, and do not become incorporated into the matrix material.

Depth-sensing indentation measurements were performed to quantify the modulus of the vitrified films. Figure 7 shows the average and standard deviation force versus displacement curves from a series of indentation measurements for the three different films. The loading portion of the curve is shown here for clarity. As reported in Table 1, the reduced moduli for the OTSE, TTSE, and TOETSE films are 5.8, 4.6, and 2.1 GPa, respectively. TOETSE showed the lowest force for a similar displacement, consistent with the harmonic contact stiffness measured by the continuous stiffness method. These moduli data strongly correlate with the average film density, and anti-correlate with the porosity, CTE, and toluene swelling data. As the average film density increases, so does the mechanical modulus. The CTE and porosity both appear to increase when the mechanical modulus decreases. These data again suggest that the general deterioration of the mechanical properties – modulus here – with increasing tether length and decreasing degree of cross-linking are rooted in changes in the porosity of the material. The fact that the lack of changes in the wall density of the solid phase does not influence the mechanical properties suggests that the porosity or packing is what governs the thermal mechanical properties such as modulus and CTE.

The surface energy of the SSQ films is influenced by both non-polar alkyl groups and polar silanol groups. It should be noted that the amount of non-polar alkyl groups can be regarded as constant regardless of the process, but the fraction of silanol groups varies significantly with temperature used for the thermal polycondensation reaction. The as-cast (non-vitrified) SSQ films are fully hydrolyzed. The high silanol content in these materials is expected to lead to very hydrophilic surfaces. As the films are heated to high temperatures and the silanols condense into a cross-linked network, the surface energy of the films decreases substantially as the silanols are consumed and the non-polar alkyl component become dominant. The static water contact angles as a function of the vitrification temperature are summarized in Fig. 8. The more extensive the vitrification process becomes, the more hydrophobic the films become. The as-cast films display a static water contact angle of approximately 70–80°. However, these films generally become very hydrophobic and display water contact angles in excess of 100° once fully vitrified. This is consistent with consumption of the silanol functionality. It is also noted that of the three materials, TOETSE generally displayed the largest water contact angles in the as-cast film, consistent with the presence of the large alkyl tethers on the cube, but this trend was reversed in the fully vitrified film. This is also consistent with the fact that some of these longer alkyl spaces thermally degrade upon vitrification, probably leading to slightly more polar degradation byproducts.

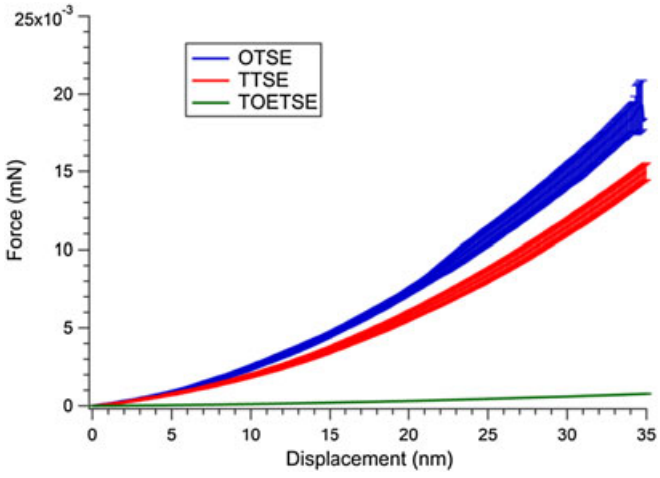

Figure 7. Force versus displacement curves during loading of the three SSQ films. The top curve is OTSE and the lower curve is TOETSE. The standard deviation is derived from multiple indents into each sample.

The results presented in this paper are consistent with our previous observations on both the processing conditions of the neat methyltrimethoxysilane (MTMS) system[15] as well as a blended system in which we add 1,2-bis(triethoxysilyl)ethane (BTSE) and vary the ratio MTMS/BTSE monomers in the initial reaction.[14] As the concentration of the closed-caged moieties in the final cross-linked SSQ network is increased, one can (i) increase the modulus and/or hardness, (ii) increase the average density, (iii) reduce the intrinsic porosity, and (iv) reduce the CTE of the SSQ film. Compared to our previous studies where we would either bias reaction conditions to minimize the formation of undesirable products, such as isolated closed-cage structures that are not incorporated into the cross-linked network, or highly branched or ladder-like structures with very little closed-cage structures, in this approach we used monomers that were only capable of forming closed-cage structures. Variations in the length and attachment density of the organic tethers that are capable of cross-linking the closed-cage SSQ moieties into the final network led to changes in the mechanical and thermal properties that are consistent with our previous observations. This approach is attractive because the final properties of the film can be tuned by properly designing the ligands for a specific target. Controlling the reaction conditions in the MTMS system can be tricky and lead to wide variations in the final properties.[14] The octameric SSQs used here lead to slightly higher cage contents in the vitrified films, as evidenced, for example, by the lower CTEs (68×10^{-6} to 93×10^{-6})°C^{-1} than our previous attempt to bias reaction conditions of MTMS towards close-cage structures, which led to higher CTEs (101×10^{-6} to 277×10^{-6})°C^{-1}.[14] Here all of the SSQ material is in the octameric form. However, by incorporating the structure-guiding BTSE momomer we were able to achieve much higher overall closed-cage and strained cyclic SSQ content. In these materials the CTE could be reduced all the way to approximately (5×10^{-6})°C^{-1}.[15] At first this might seem counterintuitive because all of the monomers utilized here are in their octameric closed-cage form. However, the difference is that the tethers used to cross-link the octameric SSQs are fairly long and comprise a significant volume fraction of the material, whereas with the BTSE cross-linking reaction the tether is just an ethyl bridge. This leads to higher density

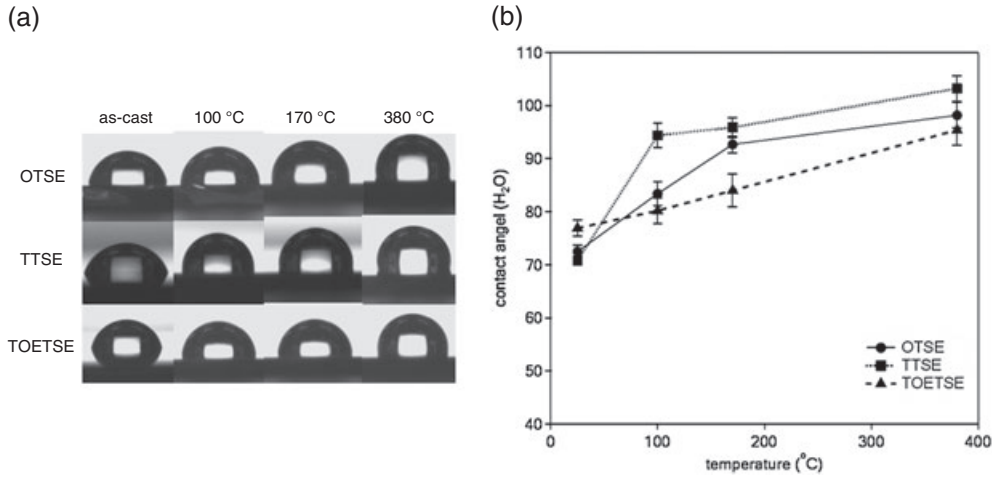

Figure 8. Part (a) shows a series of static water drops on the different film surfaces for different annealing conditions after spin casting of the SSQ film. As shown in part (b), the as-cast surfaces exhibit moderately hydrophilic surfaces due to the silanol content of the film. These surfaces, however, become very hydrophobic, showing water contact angles of the order of 100° or more after vitrification when silanols are consumed by the condensation cross-linking reaction.

of closed-cage structures and a lower CTE and higher modulus than the materials studied here. Presumably a reduction of the tether lengths for the molecules describe in Fig. 1 would be a good route to further reduce the CTE and increase the modulus and hardness of these materials and greatly enhance their tenability.

Conclusion

In this paper we have presented a series of three molecules consisting of octameric SSQ cores decorated with various organic pendent groups of variable length, end-capped to differing degrees with $Si(OEt)_3$ functional groups. We have shown that once these triethoxy end groups are hydrolyzed, the materials can be spin cast from organic casting solvents into high-quality films that can be vitrified at elevated temperatures to form optical-quality, high-modulus/hardness, low-CTE films with tunable surface energies. As the degree of cross-linking increases and/or the fraction of octameric SSQ cores in the film increases, one can realize enhancements in the mechanical and thermal properties, providing a flexible platform to generate smooth, high-modulus, chemically and thermally stable films and coatings.

References

[1] R. H. Baney, M. Itoh, A. Sakakibara, T. Suzuki, *Chem. Rev.* **1995**, *95*, 1409.
[2] R. M. Laine, *J. Mater. Chem.* **2005**, *15*, 3725.
[3] B. D. Cordes, P. D. Lickiss, F. Rataboul, *Chem. Rev.* **2010**, *110*, 2081.
[4] G. Z. Li, L. C. Wang, H. L. Ni, C. U. Pittman, *J. Inorg. Organomet. Polym. Mater.* **2001**, *11*, 123.
[5] R. Y. Kannan, H. J. Salacinski, P. E. Butler, A. M. Seifalian, *Accounts Chem. Res.* **2005**, *38*, 879.
[6] S. A. Madbouly, J. U. Otaigbe, *Prog. Polym. Sci.* **2009**, *34*, 1283.
[7] R. M. Laine, M. Roll, M. Asuncion, S. Sulaiman, V. Popova, D. Bartz, D. J. Krug, P. H. Mutin, *J. Sol-Gel Sci. Technol.* **2008**, *46*, 335.
[8] H. E. Romeo, M. Cameo, M. V. Choren, M. A. Fanovich, *J. Mater. Sci. Mater. Med.* **2011**, *22*, 935.
[9] B. Dasgupta, S. K. Sen, S. Banerjee, *Mater. Sci. Eng. B* **2010**, *168*, 30.
[10] M. Janssen, J. Wilting, C. Muller, D. Vogt, *Angew. Chem. Int. Edit.* **2010**, *49*, 7738.
[11] W. Volksen, R. D. Miller, G. Dubois, *Chem. Rev.* **2010**, *110*, 56.
[12] L. Nicole, C. Boissiere, D. Grosso, A. Quach, C. Sanchez, *J. Mater. Chem.* **2005**, *15*, 3598.
[13] Y. Toivola, J. Thurn, R. F. Cook, *J. Electrochem. Soc.* **2002**, *149*, F9.
[14] H. W. Ro, K. Char, E. C. Jeon, H. J. Kim, D. Kwon, H. J. Lee, J. K. Lee, H. W. Rhee, C. L. Soles, D. Y. Yoon, *Adv. Mater.* **2007**, *19*, 705.
[15] H. W. Ro, E. S. Park, C. L. Soles, D. Y. Yoon, *Chem. Mater.* **2010**, *22*, 1330.
[16] Certain equipment, instruments or materials are identified in this paper in order to adequately specify the experimental details. Such identification does not imply recommendation by the National Institute of Standards and Technology nor does it imply the materials are necessarily the best available for the purpose.
[17] H. J. Lee, C. L. Soles, D. W. Liu, B. J. Bauer, W. L. Wu, *J. Polym. Sci. B. Polym. Phys.* **2002**, *40*, 2170.
[18] C. Bolln, A. Tsuchida, H. Frey, R. Mulhaupt, *Chem. Mater.* **1997**, *9*, 1475.
[19] Q. R. Huang, W. Volksen, E. Huang, M. Toney, C. W. Frank, R. D. Miller, *Chem. Mater.* **2002**, *14*, 3676.